第 28 卷第 9 期 无 机 化 学 学 报 Vol.28 No.9
2012 年 9 月 CHINESE JOURNAL OF INORGANIC CHEMISTRY 1967-1978

负载于 HZSM-5 上的 $CuO-ZnO-Al_2O_3$ 纳米粒子:尿素–硝酸盐燃烧合成和理化表征

Reza Khoshbin[1,2] Mohammad Haghighi*[,1,2]
([1]Chemical Engineering Department(化学工程系), Sahand University of Technology(萨罕德工业大学), P.O.Box 51335-1996, Sahand New Town, Tabriz, Iran(伊朗)
([2]Reactor and Catalysis Research Center (RCRC)(反应器和催化研究中心), Sahand University of Technology(萨罕德工业大学), P.O.Box 51335-1996, Sahand New Town, Tabriz, Iran(伊朗))

摘要: 用尿素–硝酸盐燃烧法制备了一系列的负载于 HZSM-5 上的 $CuO-ZnO-Al_2O_3$ 纳米复合材料(CZA/HZSM-5)。研究了燃料与氧化物的比率对所合成的复合材料的理化性质的影响。用 TGA/DTG,FTIR 和 XRD 等研究了尿素–硝酸盐凝胶的热分解和煅烧粉体的相演变过程。FESEM 结果表明在燃烧过程中燃料的用量对 CZA/HZSM-5 的性质有重大影响。CuO 和 ZnO 的晶粒首先随尿素量的增加而增大,然后随尿素量的增加而减小。CuO 和 ZnO 的相对结晶度随燃料量的增加表现为非单调趋势。随着燃料与硝酸盐的比率的增加,CZA/HZSM-5 不仅形貌变得超细和均一,而且表面孔隙率也显著增加。FTIR 结果表明 HZSM-5 的结构甚至在负载了 $CuO-ZnO-Al_2O_3$ 纳米粒子后也未被破坏,而且在 CuO 和 ZnO 与 HZSM-5 之间还有表面的键合。TGA/DTG 结果指出燃烧合成法是一种由若干过程组合起来的方法,例如前驱体的热分解和前驱体间的放热反应等。另外,提出了 $CuO-ZnO-Al_2O_3$ 负载在 HZSM-5 上的生成机理。

关键词: $ZnO-CuO-Al_2O_3$; HZSM-5; 纳米复合材料; 尿素–硝酸盐燃烧合成法
中图分类号: O643.36; TQ426.6 **文献标识码**: A **文章编号**: 1001-4861(2012)09-1967-12

Urea-Nitrate Combustion Synthesis and Physicochemical Characterization of $CuO-ZnO-Al_2O_3$ Nanoparticles over HZSM-5

Reza Khoshbin[1,2] Mohammad Haghighi*[,1,2]
([1]*Chemical Engineering Department, Sahand University of Technology, P.O.Box* 51335-1996, *Sahand New Town, Tabriz, Iran*)
([2]*Reactor and Catalysis Research Center (RCRC), Sahand University of Technology, P.O.Box* 51335-1996, *Sahand New Town, Tabriz, Iran*)

Abstract: A series of $CuO-ZnO-Al_2O_3$ nanocomposites over HZSM-5 (CZA/HZSM-5) have been synthesized by urea-nitrate combustion method. The influence of the fuel to oxidant ratio on the physicochemical properties of synthesized nanocomposites has been studied. The thermal decomposition of urea-nitrate gels and the phase evolution of calcined powder were investigated by TGA/DTG, FTIR and XRD techniques. The FESEM results show that the properties of the CZA/HZSM-5 are significantly influenced by fuel content used in the combustion process. The crystalline size of the CuO and ZnO initially increases with the increase in urea content and then decreases with further addition of urea. The relative crystallinity of CuO and ZnO shows non monotonic trend with increasing of fuel content. With increasing of fuel to nitrate ratio, not only the morphology of the CZA/

收稿日期:2011-12-17。收修改稿日期:2012-04-16。
*通讯联系人。E-mail:haghighi@sut.ac.ir, Tel: +98-412-3458097 & +98-412-3459152, Fax: +98-412-3444355, web: http://rcrc.sut.ac.ir。

HZSM-5 becomes ultra-fine and homogeneous, but also the surface porosity increases obviously. FTIR results show that HZSM-5 structure is not damaged even after loading with CuO-ZnO-Al_2O_3 nanoparticles and there are external linkages between CuO and ZnO with HZSM-5. TGA/DTG curves indicate that the combustion synthesis method is a combination of several phenomena such as thermal decomposition of precursors and exothermal reactions between them. Furthermore, a formation channel of CuO-ZnO-Al_2O_3 over HZSM-5 was proposed.

Key words: ZnO-CuO-Al_2O_3; HZSM-5; nanocomposite; urea-nitrate combustion

0 Introduction

Recently, nanomaterials have been prepared and received great attention because of their potential role in basic scientific research and fabricating nanodevices with novel optical, electrical and chemical properties [1-2]. Various preparation methods toward diverse nanomaterials, including precipitation, sol-gel, impregnation, sonochemical, templating direction, solution-based solvothermal or hydrothermal treatment and combustion synthesis method have been extensively developed [3-4]. Among these, combustion method is an easy and convenient method for preparation of a variety of advanced ceramics, catalysts and nanomaterials.

In recent years, the CuO-ZnO-Al_2O_3 (CZA) nanocomposites are gaining a great importance. It has been doped over variety of supports and widely employed as catalyst in direct conversion of syngas to dimethyl ether reaction[5], steam reforming of dimethyl ether in fuel cells [6] and other industrial potential applications[7-9]. Among various substrates, zeolites (for example HZSM-5) have high surface area, high thermal stability and eco-friendly nature. Moreover, zeolites possess amphoteric properties, Lewis-acidity to denote electron-accepting ability and Lewis basicity to describe electron-donating property [10]. Various routes have been employed for CZA production such as co-precipitation [11], sol-gel preparation [12], impregnation [13]and physically mixing[14]. Although the precipitation method improves reactivity of the components, the incomplete precipitation leads to alternation of stoichiometry and the chemical homogeneity cannot be readily obtained due to differences in the solubility or complex formation between various chemical species [15]. The sol-gel technique requires expensive precursors [16], while in impregnation and physically mixing methods, dispersion of CZA over HZSM-5 is low. On the other hand, most of these methods cannot be applied to a large scale and economical production because they require expensive and often toxic reagents, high reaction temperature as well as long reaction time. One of the nanostructure synthesis methods is the combustion reaction which stands out as an alternative and highly promising method for the synthesis of nanostructured materials [17,18]. The resulted product is usually in a crystalline form. It is dry agglomerated into highly fluffy foam with high chemical homogeneity and purity.

The combustion route is composed of gelling and subsequent combustion of the solution. It contains nitrates salts and some organic fuels, such as urea[19], citric acid [20], glycine [21], ethylene glycol [22], etc. The mixture starts boiling, then it ignites and an exothermal, selfsustaining and very fast chemical reaction occurs, resulting in a dry, usually crystalline, fine oxide powder. In this method rapid evolution of a large volume of gases during the process immediately cools the product and limits the occurrence of agglomeration[16]. Since urea is commercially available, cheap and generates the highest temperature during combustion, it seems to be as one of the best suitable organic fuel[23].

Most of the previous investigations reported in the literature focus on the properties of final products

and effect of composition of the reactant mixture on both phase composition and microstructure of the products. However, very little literature is available in which the effect of non-nitrate precursors such as zeolites on the structural properties of final products has been investigated[24-26].

Since heat induced from the reactions strongly depends on fuel to nitrate ratio, the finding of a suitable ratio of oxidant to fuel is very important. A non-suitable ratio of fuel to nitrate makes some unwanted intermediate phases or unreacted raw materials[27]. Therefore, in this paper the applicability of the urea-nitrate combustion method for synthesis of powders in the presence of non-nitrate precursor (HZSM-5) is studied. Furthermore, the role of the fuel to metal nitrates ratio on physicochemical properties of the nano composite has been investigated by XRD, BET, FESEM, FTIR and TGA/DTA techniques and the combustion behaviors described as well.

1 Experimental

1.1 Materials

Analytic grade chemicals of copper nitrate ($Cu(NO_3)_2\cdot 3H_2O$), zinc nitrate ($Zn(NO_3)_2\cdot 3H_2O$), aluminium nitrate ($Al(NO_3)_3\cdot 9H_2O$), ammonium nitrate (NH_4NO_3), ammonia (NH_3(33%)) and urea ($CO(NH_2)_2$) were supplied by Merck, while NaZSM-5 with Si/Al=21 obtained from SPAG. All of them used as received without any further purification.

1.2 Preparation and procedures

The experimental procedure for preparation of CZA/HZSM-5 nanocomposite is schematically shown in Fig.1. As illustrated in the flow diagram, the preparation of the nanocompositeis divided into 3 stages. In stage (a), HZSM-5 sample was prepared from an original NaZSM-5 powder by repeated ion exchange with NH_4NO_3 solutions followed by drying overnight and calcinations in air at 550 ℃ for 5 h. In stage (b), appropriate amount of $Cu(NO_3)_2\cdot 3H_2O$ and $Zn(NO_3)_2\cdot 3H_2O$ and $Al(NO_3)_3\cdot 9H_2O$, in a molar ratio of Cu:Zn:Al 6:3:1, were dissolved in a minimum amount of deionized water. After magnetic stirring for 15 min, a transparent solution was formed. In last stage (c), urea was added into the solution. The mixed solution was neutralized to pH=7 by adding liquor ammonia. Then the neutralized solution was evaporated to dryness by heating at 100 ℃ on a hot plate with continuous stirring. As water evaporated, the solution became viscous and finally formed a very viscous deep blue gel. The resultant gel was transferred into ceramic crucible and subjected to combustion reaction in a preheated electric furnace maintained at 350 ℃.

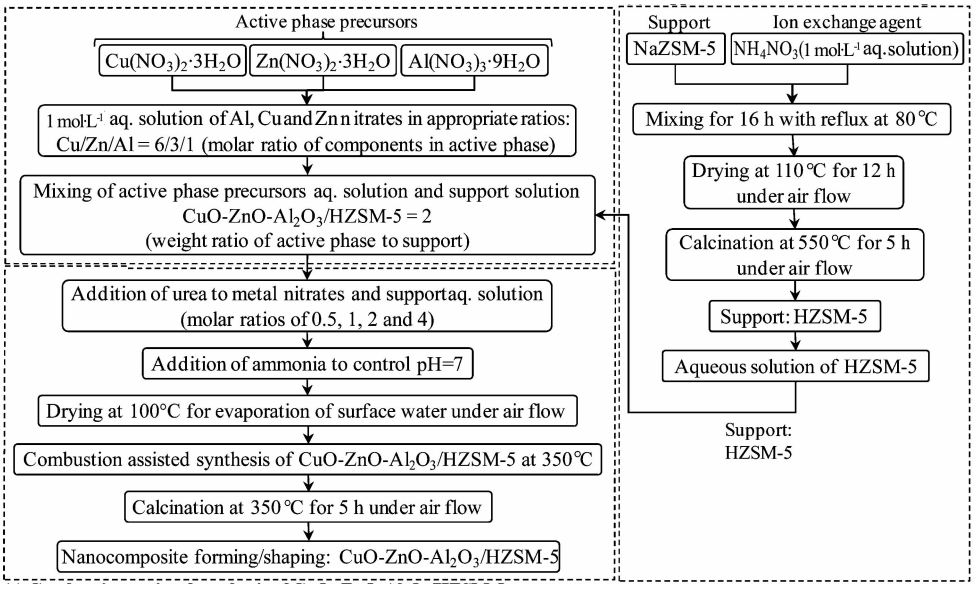

Fig.1 Schematic flow chart for the preparation steps of CZA/HZSM-5 nanocomposite via urea-nitrate combustion method

The gel started boiling and in a couple of minutes ignited spontaneously with rapid evolution of large quantity of gases, yielding a foamy, voluminous powder. In order to burn-off carbon residues, the powders were further heated at 350 ℃ for 5 h. For addressing of the effect of urea content, four samples were prepared with different molar ratios of 0.5, 1, 2 and 4 (urea to nitrates).

1.3 Characterizations

Powder X-ray diffraction (XRD) measurements were performed using a Siemens diffractometer D5000 with a Cu-$K\alpha$ radiation source (λ =0.154 06 nm) operating at 40 kV and 30 mA in a scanning range of 5°~70° (2θ). The diffraction peaks of the crystalline phase were compared with those of standard compounds reported in the Joint Committee of Powder Diffraction Standards data base (PDF). The crystallite size of CuO, ZnO, and HZSM-5 of the calcined nanocomposites were evaluated from full width at half maximum of the XRD peaks using Scherrer algorithm. The microstructure and morphology was studied by field emission scanning electron microscopy (HITACHI S-4160). Specific surface area analyses were carried out using BET (Brunauer, Emmett, and Teller) technique by Quantachorom CHEMBET apparatus. Furthermore, thermo gravimetric analyzer (Perkin Elmer TGA/DTG) was used to determine the mass loss of the nanocomposite as a function of increasing of temperature. The samples were heated up to 500 ℃ at 10 ℃·min^{-1} in an aluminum crucible under air flow. The DTG profiles were obtained by differentiating the TGA profiles. Finally, for addressing surface functional groups, the nanocomposite mixed with KBr and characterized withUNICAM 4600 Fourier Spectrometer in a range of 400~4 000 cm^{-1}.

2 Results and discussion

2.1 Nanocomposite characterizations

2.1.1 Crystallographic analysis

XRD patterns of the ZSM-5 and synthesized nanocomposites with different urea/nitrates ratio are

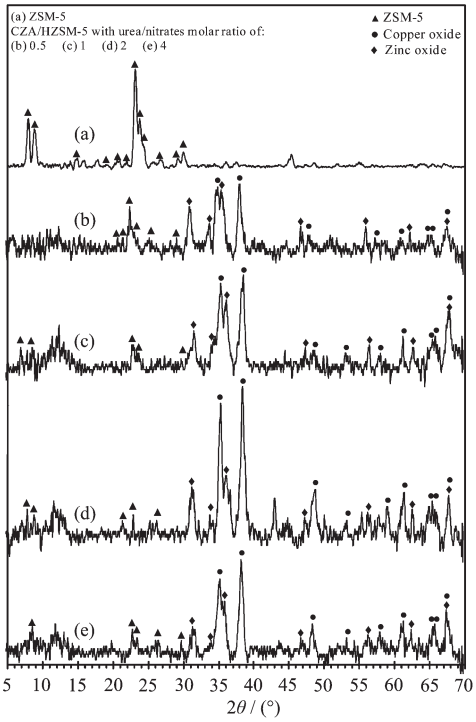

Fig.2 XRD patterns of (a) ZSM-5 and CZA/HZSM-5 nanocomposite synthesized via urea-nitrate combustion method at different urea/nitrates molar ratios of (b) 0.5, (c) 1, (d) 2 and (e) 4

shown in Fig.2. One can see that with increasing of urea content in the reaction mixture, the diffraction peaks become narrower, while the intensity of peaks initially increases and then decreases.

In the XRD patterns, there are rather strong peaks at 2θ=35.6° and 38.8° that can be assigned to CuO and indexed to the monoclinic phase of CuO (PDF No.01-080-1268) with Miller indexes of (111) and (111), respectively. Furthermore, it can be seen, with increasing of urea content, the CuO peaks at 48.7° and 68.2° appear. The peaks at 2θ=31.96° and 36.25° are ascribed to hexagonal phase of ZnO (PDF No.01-076-0704) with Miller indexes of (100) and (101), respectively. It is observed that some of the CuO and ZnO peaks have overlap. For example, the peak of ZnO at 2θ=36.25° is severely covered by the peak of CuO at 2θ=35.6°. As shown in Fig.2 (a), the substrate ZSM-5 exhibits representative reflections at both low-angle (2θ<10°) and high-angle (20°<2θ<60°) ranges. Due to high degree of HZSM-5 coating with oxides nanocomposite, it is observed that some of the

low angle diffraction peaks of HZSM-5 decrease and have not certain trend with increasing of urea content.

There is no shift for the position of HZSM-5 diffraction peaks in the CZA/HZSM-5 nanocomposite. This shows that the addition of CuO-ZnO-Al_2O_3 has no effect on the crystalline lattice of HZSM-5. The XRD patterns show that HZSM-5, CuO and ZnO are the main components of the nanocomposite. It is worth pointing out that, there are no peaks that can be assigned to Al_2O_3. This observation suggests that Al_2O_3 is highly dispersed and/or is amorphous which is in line with the previous observation in the literature[28].

The crystallite sizes of CuO and ZnO particles are measured using the Scherrer algorithm and plotted in Fig.3. As can be seen, the calculated crystallite sizes of CuO are 31.6, 31.4, 39.4 and 39.5 nm, for urea/nitrates ratio of 0.5, 1, 2 and 4, respectively. The results indicate that with increasing of urea content from 0.5 to 4, the crystallite size of ZnO increases from 30.4 nm to 40.5 nm, respectively. The thermal energy due to organic material decomposition leads to the increase in the crystal size. This increase in the crystallite size is attributed to increase in the reaction temperature and time of combustion process as the fuel ratio increases.

The relative crystallinity of synthesized CZA/HZSM-5 nanocomposite at different urea/nitrates molar ratios are plotted in Fig.4. As can be seen, the relative crystallinity of CuO initially increases from

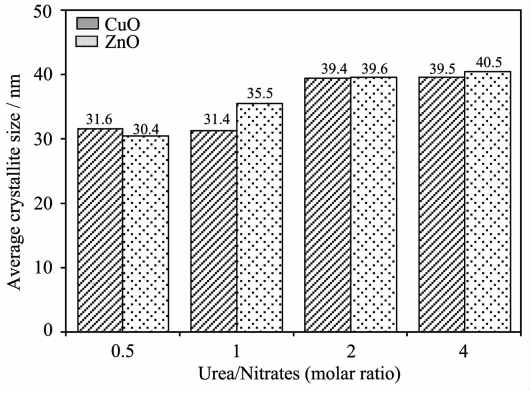

Fig.3 Estimation of average crystallite size of oxides phases using Scherrer algorithm for synthesized CZA/HZSM-5 nanocomposite at different urea/nitrates molar ratios of 0.5, 1, 2 and 4

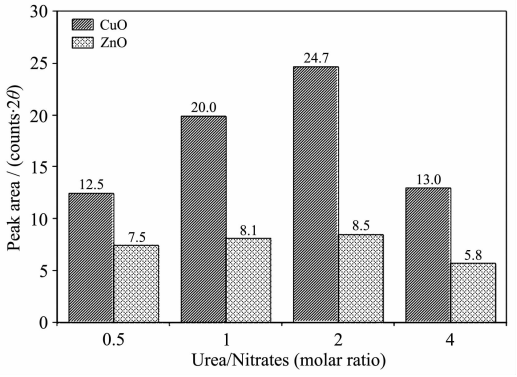

Fig.4 Estimation of relative crystallinity of synthesized CZA/HZSM-5 nanocomposite at different urea/nitrates molar ratios of 0.5, 1, 2 and 4

12.5 (urea to nitrate ratio=0.5) to 24.7(urea to nitrate ratio =2) and then decreases to 13 (urea to nitrate ratio =4). Moreover, there is the same trend for crystallinity of ZnO. This can be possibly addressed by slow nucleation rate and high growth rate at higher temperature. Singh et al. [29] demonstrated a similar variation in crystallite size with increase in fuel content when they used the citrate-nitrate process for the preparation of YSZ particles.

2.1.2 Morphological analysis

Fig.5 shows the FESEM images of the zeolite and CuO-ZnO-Al_2O_3 nanocomposite grown on HZSM-5 substrates at different urea to nitrate ratios. This figure shows a clear change in morphology as the fuel content in the combustion increases from 0.5 to 4 times of stoichiometric ratio.

As can be seen in Fig.5 (a), the morphology of HZSM-5 is cubic; while the sample with urea to nitrate ratio of 0.5, exhibits a flower-like morphology and high degree of aggregation of particles. When stoichiometric amount of urea is used, irregularly shaped agglomerate with a few pores is observed. The sample with urea to nitrate ratio of 2 shows the same morphology when the urea to nitrate ratio is set to 4, porous morphology appears. The last sample is more porous and looser than the others due to more gases released in the combustion process.

As discussed in XRD patterns, the removal of volatile masses during the combustion plays a

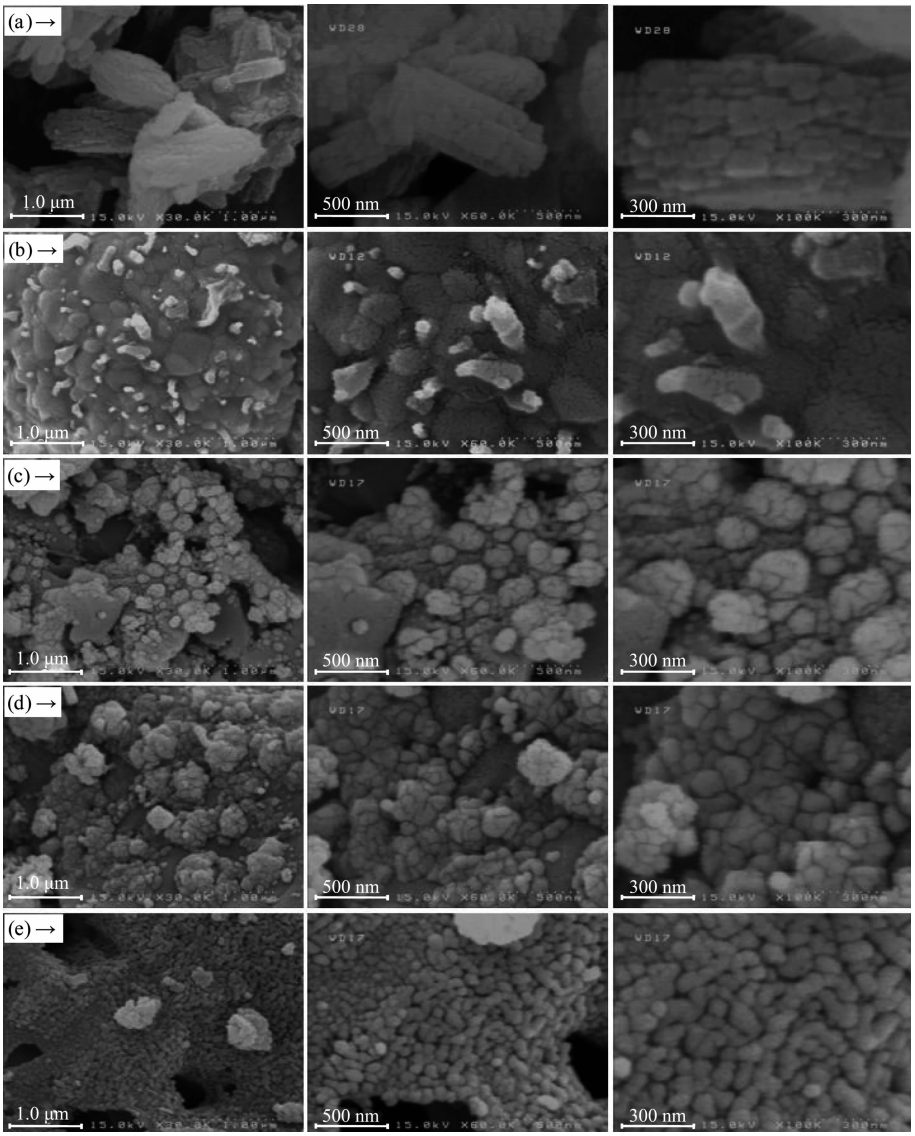

Fig.5 SEM images of (a) ZSM-5 and CZA/HZSM-5 nanocomposite synthesized via urea-nitrate combustion method at different urea/nitrates molar ratios of (b) 0.5, (c) 1, (d) 2 and (e) 4

significant role on the variation of crystallite sizes and relative crystalinity. The polymeric distribution and its subsequent removal during combustion process are expected to control the particle growth and the final morphology of the particles. Enhancement of urea to nitrate ratio from 0.5 to 4, results in slower decomposition of the salts and incomplete combustion of the urea ions. Therefore, a lot of carbonaceous matter is left in the as-prepared powder. During calcination, the removal of gaseous products from the precursor gives rise to capillary forces on the particles, which brings more particles to be exposed to each other. This results in more particle agglomeration, cluster formation and particle growth during synthesis. Consequently, the crystallite size of nonocomposites increases with increasing the urea content. Further increase in urea content (e.g. 4) leads to larger separation between the composite particles. In fact, the presence of excess urea plays the role of a space-filling template and the CZA particles surrounded in matrix become crystalline. This increase in the diffusion distance seems to be the actual reason for decreasing of particle size upon further increase in urea content.

The results suggest that high urea content decreases the agglomeration of CuO-ZnO-Al_2O_3

powders, which are beneficial for highly homogeneous powder morphology. Furthermore, since existence of well dispersed and strongly interacting between the ZSM-5 surface and CZA species, one can expect that samples prepared by the urea-nitrates combustion method will have better catalytic performance.

Fig.6 illustrates the detailed analysis of FESEM images for CZA/HZSM-5 nanocomposite synthesized via urea-nitrate combustion method with urea to nitrate ratio of 4. As mentioned above, CZA/HZSM-5 nanocomposite can be used as the catalyst in many chemical processes. In addition to the positive effect of nano-size distribution of active phase, the large values of pores are beneficial by facilitating mass-transfer of reactants and products beside the additional promotion of high concentration of active site formation. As depicted in this figure, with urea to nitrate ratio of 4, the achievement of nano-size distribution of CZA on HZSM-5 and high porous structure are obtained simultaneously.

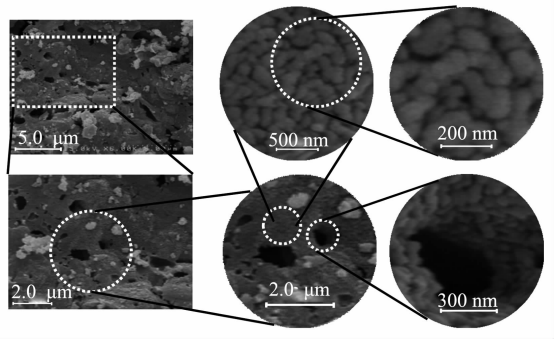

Fig.6 Detail analysis of SEM images of CZA/HZSM-5 nanocomposite synthesized at urea/nitrates molar ratio of 4

Further analysis has been carried out to address size distribution histogram of combustion pores of the same sample (Fig.7). According to this figure, CZA/HZSM-5 nanocomposite shows a monomodal pore size distribution with macrospore size around 0.475 μm possibly attributed to the releasing of gas during combustion. Further investigation shows that the dimensions of 87.9% of pores are below 1 μm. Moreover, the dimensions of the largest and the smallest pores are 2.65 and 0.155 μm, respectively.

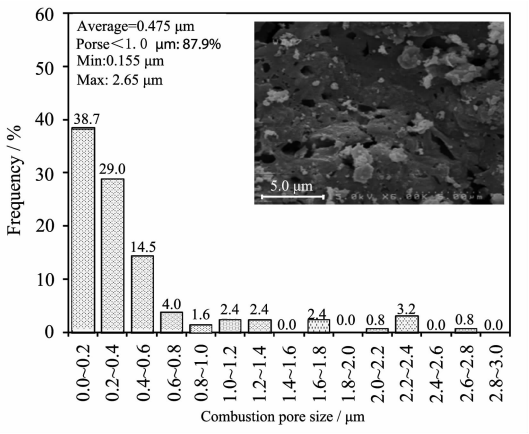

Fig.7 Size distribution histogram of combustion pore of CZA/HZSM-5 nanocomposite synthesized at urea/nitrates molar ratio of 4

Fig.8 shows the size distribution histogram of the nanocomposite with urea to nitrate ratio of 4. The particles size is distributed between 43.9~177.8 nm with standard deviation of 27.6. The average size of metal oxide phase is 80.79 nm in which 69.5% of the particles are below 100 nm. It can be seen that the powder prepared through urea route has nanometric particles with monomodal distribution as 37.1% of nanocomposite is in the range of 60~80 nm.

2.1.3 Surface area analysis

The specific surface area of ZSM-5 and synthesized CZA/ZSM-5 nonocomposites are shown in Fig.9. The specific surface areas of the nanocomposite are smaller than the substrate. With increasing of urea content, the area initially decreases then increases

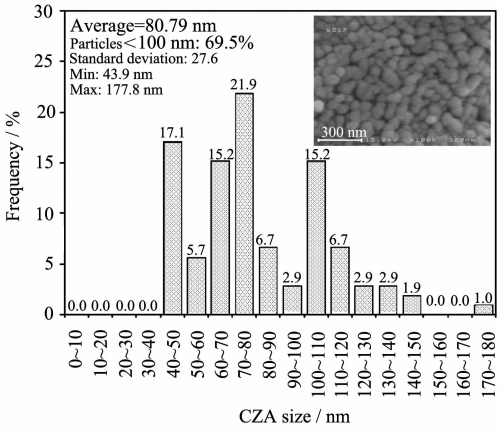

Fig.8 Size distribution histogram of CZA/HZSM-5 nanocomposite particles synthesized at urea/nitrates molar ratio of 4

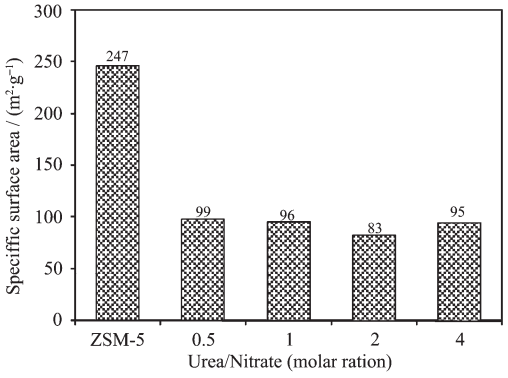

Fig.9 Specific surface area of ZSM-5 and CZA/HZSM-5 nanocomposite synthesized via urea-nitrate combustion method at different urea/nitrates molar ratios of 0.5, 1, 2 and 4

with a maximum of 99 $m^2 \cdot g^{-1}$ when urea to nitrate ratio is 0.5.

This result is in good agreement with the results regarding relative crystallinity, as determined from XRD patterns in which relative crystallinity increases with increase in ure acontent until it reaches 2, then decreases at ratio of 4.

The effect of urea to nitrate ratio on the surface area is in contrast to what is observed in FESEM analysis. When high urea content is employed, larger amount of gases is evolved during combustion and it is expected that specific surface area and porosity of nanocomposite is increased. It should be noted that CZA nanocomposite synthesized by conventional methods has average surface area of 85 $m^2 \cdot g^{-1}$ [30]. Therefore, the high surface area in these samples could be addressed by high surface area of zeolite. When fuel to nitrate ratio is increased, the relative crystallinity of nanocomposite is increased. Conseq-uently the pores of ZSM-5 are covered. In spite of microspores morphology, this plugging is very strong so that the sample with high urea content has lower surface area.

2.1.4 FTIR analysis

The FTIR spectra of ZSM-5 and synthesized CZA/HZSM-5 nanocomposites via different urea contents are shown in Fig.10. As can be seen in Fig. 10 (a), the FTIR spectrum of ZSM-5 shows bands at 455, 555, 800, 1095, 1 228 and 1 400 cm^{-1}, which are assigned to different vibrations of tetrahedral and framework atoms in HZSM-5 zeolite[31]. The ratio of the intensities of bands at 455 and 555 cm^{-1} provides an approximation to estimate of the degree of crystallinity of a given zeolite sample[32]. With increasing of the urea content, this ratio is decreased; however, in sample with urea to nitrate ratio of 4 it is increased slightly. Furthermore the band at 555 cm^{-1} indicates the formation of the five membered ring of the pentasil zeolite structure by tetrahedral SiO_4 and AlO_4 units[33]. The band at 1 228 cm^{-1} is assigned to external asymmetric stretching vibration of four chains of five member rings disposed around a double helix[34]. The bands observed at 455 and 555 cm^{-1} are characteristic of Cu-O and Zn-O vibration band, respectively, that some of them have overlap with HZSM-5 frequency band[35-36]. The broad band at 3 450 cm^{-1} is attributed to the hydroxyl groups, which are extensively hydrogen bonded. The band at *ca.* 1 645 cm^{-1} is assigned to the bonding vibrational mode of the interlayer water molecules[37].

The strongest peak at 1 095 cm^{-1} is assigned to the framework stretching vibration band of Si(Al)-O in

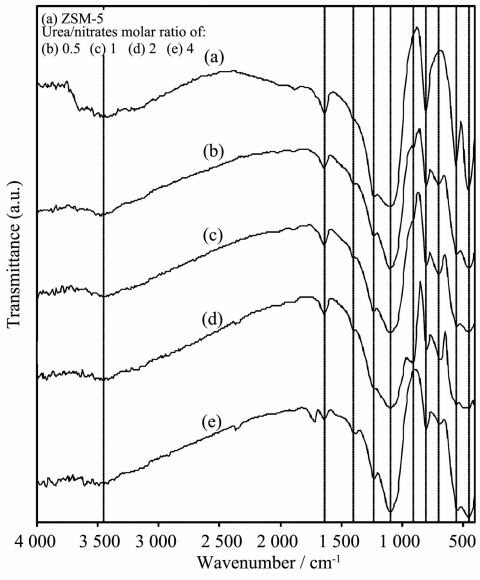

Fig.10 FTIR spectrum of (a) ZSM-5 and calcinated CZA/HZSM-5 nanocomposite synthesized via urea-nitrate combustion method at different urea/nitrates molar ratios of (b) 0.5, (c) 1, (d) 2 and (e) 4

tetrahedral $Si(Al)O_4$ in ZSM-5[34]. The position of this band remains almost unchanged in all of nanocomposites, indicating that HZSM-5 structure is not destroyed even after it is loaded with CZA nanoparticles. Furthermore, not any characteristic band is observed for other impurities such as $Cu(OH)_2$ or $Zn(OH)_2$ in FTIR patterns. These results support and complement the XRD data.

The obvious bands at 905 cm^{-1} due to Cu-O and Zn-O perturbations of asymmetric internal zeolite stretching vibrations are observed in sample b, c and d. Therefore, with increasing of urea content until 2, there is significant chemical interaction between CuO and ZnO with ZSM-5[38]. Furthermore, as can be seen in Fig.10(e), there is no chemical interaction between CuO and ZnO with ZSM-5 but there is asymmetric stretch vibration of the T-O bond at 1 235 cm^{-1} which can be assigned to external linkages between TO_4 tetrahedral [33]. This result indicates that the nature of the band between CuO and ZnO with HZSM-5 changes significantly with increasing of urea content from 2 to 4.

IR spectra of the gel before and after calcinations were examined to investigate the chemical and structural changes that take place during the combustion process. As can be seen in Fig.11, after calcinations, many of the bands related to organic materials are eliminated. The IR spectrum of noncalcined sample indicates the presence of carbonate ions. The strong band at 1 400 and 1 500 cm^{-1} originates from the CO_3^{2-} ion. The IR bands observed below 1 000 cm^{-1} can be attributed to carbonate and the metal hydroxyl modes (M=Cu, Zn and Al)[39-40].

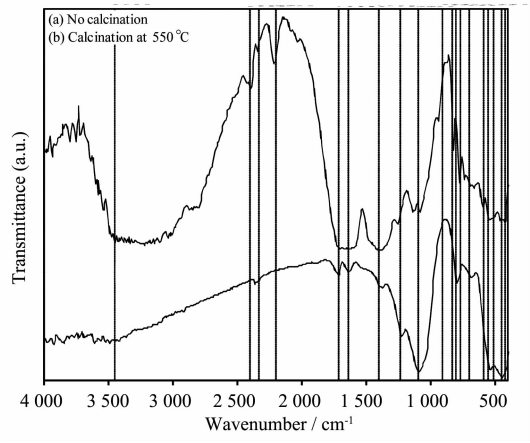

Fig.11 FTIR spectrum of CZA/HZSM-5 nanocomposite synthesized via urea-nitrate combustion method at urea/nitrates molar ratio of 4 (a) before and (b) after calcination at 350 ℃

Furthermore, the calcination reduced the intensities in the region of 3 400~3 700 cm^{-1} for nanocomposite. The disappearance of bands with a wave number larger than 3 625 cm^{-1} is attributed to condensation reactions occurred between different kinds of hydroxyl groups during calcination at 350 ℃.

2.1.5 Thermogravimetric analysis

The TGA/DTG results for the urea-nitrate dried gels prepared with different ratios of nitrates to urea are shown in Fig.12. It can be seen that there is a sharp weight loss in each case that indicates the occurrence of combustion reaction.

All of the TGA curves demonstrate three weight loss steps except for the gel with urea to nitrate ratio of 4 that has shown four weight loss steps. In all samples, the slight continuous weight loss at lower temperatures up to 150 ℃ is attributed to the gradual evaporation of absorbed water and dehydration reaction of the gels (Zone Ⅰ). In Fig.12(a) and(b), the weight loss from 150 to 230 ℃ is due to the decomposition of different nitrates and ammonium nitrate accompanied by significant weight loss (Zone Ⅱ). The sharp exothermic peak in DTG curve in a very narrow temperature range of 240~260 ℃ can be attributed to the reaction of nitrates with urea resulting in a sharp weight loss in TGA plot with 50% weight loss (Zone Ⅲ). With increasing the urea content, the second weight loss zone shifts to 250 ℃ and becomes deeper and the third weight loss zone becomes weaker.

The small broad peak at about 370 ℃ is due to the complete oxidation of residual carbon in the sample accompanied by approximatly 10% weight loss. On the other hand, in the sample with urea to metal nitrate ratio of 0.5, there is no weight loss after the combustion reaction. This indicates complete

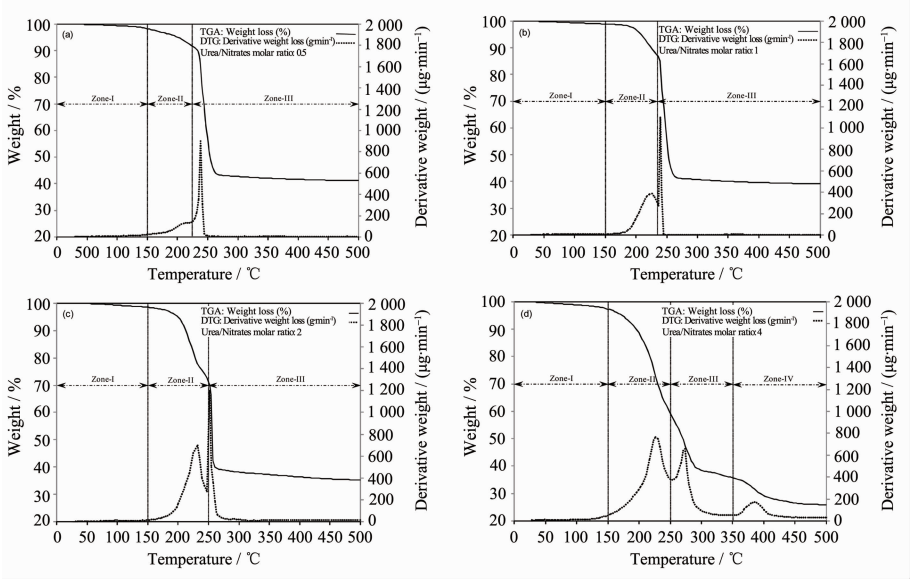

Fig.12 TG-DTG analysis of CZA/HZSM-5 nanocomposite synthesized via urea-nitrate combustion method at different urea/nitrates molar ratios of (a) 0.5, (b) 1, (c) 2 and (d) 4

combustion reaction giving a product free of residual reactants and carbonaceous matter.

It can be seen that the decomposition process in samples with a high urea ratio is associated with slow rate of weight loss during heating as compared to those in samples with lower ratio of urea, which decomposes rapidly. With increasing the urea to nitrate ratio, the concentration of nitrate ions in the sample decreases. Due to the decrease of oxidant, the rate of redox reaction is decreased, and the ignition temperature is increased.

Therefore, it could be addressed that the combustion rate is affected by the molar ratio of urea to metal nitrate in which the highest rate is achieved with the urea to nitrate molar ratio of 0.5.

2.2 Reaction channels for CuO-ZnO-Al_2O_3 formation over HZSM-5

The molar ratio of fuel to metal nitrate has been determined based on the propellant chemistry principal. Hence, reducing valences of nitrogen and carbon have been taken as 0 and 4, respectively. Furthermore, it should be considered that N_2 and CO_2 are the gaseous combustion products. Presence of these gaseous states in the evolved combustion product has been reported in the literature [41]. Therefore, the overall reaction between nitrate precursors and urea during the combustion process can be represented as follows:

$$0.6Cu(NO_3)_2\cdot 2H_2O+0.3Zn(NO_3)_2\cdot 6H_2O+0.1Al(NO_3)_3\cdot 9H_2O+mCO(NH_2)_2 \rightarrow (CuO)_{0.6}(ZnO)_{0.3}(Al_2O_3)_{0.5}+(m+1.05)N_2+(2m+4.5)H_2O+CO_2 \quad (1)$$

Though the amount of nitrate ions in the solution is less, the redox mixture generates sufficient exothermic heat for the evolution of the precursors into metal oxides and produces a large amount of gases in a short period of time that keeps the powder well dispersed in large volume.

In gel synthesis process, urea is not only employed as a fuel, but partially decomposed to ammonia and water to maintain the constancy of the pH value of the solution during the evaporation process. In this process, the combustion wave propagates from first to the end of the reactant and the combustion reaction is completed within a few minutes. There are some mechanisms to describe what occurs in combustion process.

For this case, at first, urea decomposes initially to HCNO (reaction 2) and, metal nitrate decomposes to metal hydroxide and nitric acid (reactions 3~5). Ammonia solution is used to adjust pH value to 7.

Simultaneously, ammonia solution reacts with the nitric acid to form ammonium nitrate, which could be used as an oxidizer (reactions **6~7**). The colored gel is due to the formation of chelate complexes between the biuret (which is a bidentate ligand, coordinates through the terminal nitrogens) and the metal ions. This complex prevents from the precipitation of metal hydroxide groups (reaction **8~10**).

Then final gas phase reactions between combustible species (like ammonia and above complex) and oxides of nitrogen occur and lead to the appearance of a flame. This phenomenon can be attributed to strong oxidation-reduction reaction in combustion, which can be proved by the TGA/DTG analysis. Simultaneously, the massive reaction heat results in the reaction of highly reactive CuO-ZnO-Al_2O_3 with HZSM-5 to yield CZA/HZSM-5 nanoparticles as observed in reaction (**1**). For better understanding the mechanism of combustion synthesis, a calorimetric study with the simultaneous analysis of gaseous reaction products is recommended for future studies.

$$CO(NH_2)_2 \xrightarrow{-NH_3} HCNO \xrightarrow{+urea} C_2H_5N_3O_2 \quad (2)$$

$$Cu(NO_3)_2 \xrightarrow{H_2O} Cu(OH)_2+HNO_3 \quad (3)$$

$$Zn(NO_3)_2 \xrightarrow{H_2O} Zn(OH)_2+HNO_3 \quad (4)$$

$$Al(NO_3)_3 \xrightarrow{H_2O} Al(OH)_3+HNO_3 \quad (5)$$

$$NH_4OH \rightarrow NH_3+H_2O \quad (6)$$

$$NH_3+HNO_3 \rightarrow NH_4NO_3 \quad (7)$$

$$Cu(OH)_2+C_2H_5N_3O_2 \rightarrow Cu(C_2H_5N_3O_2)_2^{2-}+2OH^- \quad (8)$$

$$Zn(OH)_2+C_2H_5N_3O_2 \rightarrow Zn(C_2H_5N_3O_2)_2^{2-}+2OH^- \quad (9)$$

$$Al(OH)_3+C_2H_5N_3O_2 \rightarrow Al(C_2H_5N_3O_2)_2^{2-}+3OH^- \quad (10)$$

3 Conclusions

The combustion method is a simple and fast route for the synthesis of ultrafine, nanocrystalline CZA/HZSM-5 composite. The combustion processes and physicochemical properties of composite are greatly influenced by the urea content. The combustion rate is the most vigorous and rapid for the gel with urea to nitrate ratio of 0.5. Results from the TGA/DTG curves show that a drastic combustion reaction occursat around 250 ℃. It is observed that the products are homogenous and crystalline. XRD patterns show that CuO, ZnO are formed on HZSM-5 substrate. Moreover, the amount of urea plays an important role on the control of particle size. The calcined powders are spherical in shape and their particle sizes in the sample with urea to nitrate ratio of 4 are in range of 20~100 nm.

Acknowledgements: The authors gratefully acknowledge Sahand University of Technology for the financial support of the project as well as Iran Nanotechnology Initiative Council for complementary financial support.

References:

[1] Burda C, Chen X, Narayanan R et al. *Chem. Rev*., **2005**,**105**(4):1025-1102
[2] Ying Jackie J. *Chem. Eng. Sci.*, **2006**,**61**(5):1540-1548
[3] Li X, Liu H, Han F, et al. *Mater. Sci. Eng. A*, **2004**,**379**(1/2):347-350
[4] Abbasi A R, Morsali A. *Ultrason. Sonochem*., **2010**,**17**(4):704-710
[5] Zhao Y, Chen J, Zhang J. *J. Nat. Gas Chem*., **2007**,**16**(4):389-392
[6] Tanaka Y, Kikuchi R, Eguchi K, et al. *Appl. Catal. B*, **2005**, **57**(3):211-222
[7] Sá S, Sousa J M, Mendes A. *Chem. Eng. Sci*., **2011**,**66**(20):4913-4921
[8] Chang C C, Chang C T, Chen Y, et al. *Int. J. Hydrogen Energy*, **2010**,**35**(15):7675-7683
[9] Huang G, Liaw B J, Chen Y Z, et al. *Appl. Catal. A*,**2009**, **358**(1):7-12
[10]Ökte A N, Ylmazö. *Appl. Catal. A*, **2009**,**354**(1/2):132-142
[11]Sun K, Lu W, Xu X, et al. *Appl. Catal. A*, **2003**,**252**(2):243-249
[12]Moradi G R, Nosrati S, Yaripor F. *Catal. Commun.*, **2007**,**8**(3):598-606
[13]Ahn S H, Kim S H, Jung K B, et al. *Korean J. Chem. Eng*., **2008**,**25**(3):466-470
[14]Mao D, Yang W, Chen Q. *J. Catal*., **2005**,**230**(1):140-149
[15]Veith M, Mathur S, Huch V, et al. *J. Mater. Chem*., **1999**,**9**(12):3069-3079
[16]Avgouropoulos G, Ioannides T. *Appl. Catal. A*, **2003**,**244**(1):155-167
[17]ZanettiS M, Santiago E I, Longo E, et al. *Mater. Lett.*, **2003**, **57**(19):2812-2816

[18]Si Y C, Jiao L F, Yuan H T, et al. *J. Alloys Compd*., **2009**, **486**(1/2):400-405

[19]Naik M A, Mishra B G, Dubey A. *Colloids Surf. Physicochem. Eng. Aspects*, **2008**,**317**(1/2/3):234-238

[20]Zhu J, Xiao D, Li J, et al. *Scripta Mater.*, **2006**,**54**(1):109-113

[21]Lenka R K, Mahata T, Sinha P K, et al. *J. Alloys Compd*., **2008**,**466**(1/2):326-329

[22]Chen W, Li F, Yu J. *MatL*, **2007**,**61**(2):397-400

[23]Costa A C F M, Morelli M R, Kiminami R H G A. *J. Mater. Synth. Process*, **2001**,**9**(6):347-352

[24]Li J, Pan Y, Guo J, et al. *Ceram. Int*., **2007**,**33**(6):1047-1052

[25]Mir M, de Paula C C, Mascarenhas Y P, et al. *J. Eur. Ceram. Soc*., **2007**,**27**(13/14/15):3719-3721

[26]Amarilla J M, Petrov K, Rojas R M, et al. *J. Power Sources*, **2009**,**191**(2):591-600

[27]Riahi-Noori N, Sarraf-Mamoory R, Mehdikhani A, et al. *J. Ceram. Process. Res*., **2008**,**9**(3):246-249

[28]Zhang X, Zhong L, Xie K, et al. *Fuel*, **2010**,**89**(7):1348-1352

[29]Singh K A, Pathak L C, Roy S K. *Ceram. Int*., **2007**,**33** (8):1463-1468

[30]FENG Dong-Mei(冯冬梅), ZUO Yi-Zan(左宜赞), WANG Jin-Fu(王金福), et al. *Chinese J. Catal.*(*Cuihua Xuebao*), **2009**,**30**(3):223-229

[31]Othman Ali I. *Mater. Sci. Eng., A*, **2007**,**459**(1/2):294-302

[32]Ali M A, Brisdon B, Thomas W J. *Appl. Catal. A*, **2003**,**252** (1):149-162

[33]Cheng Y, Wang L J, Sun X Y, et al. *Mater. Lett.*, **2005**,**59** (27):3427-3430

[34]Barros I C L, Braga V S, Pinto D S, et al. *Microporous Mesoporous Mater*., **2008**,**109**(1/2/3):485-493

[35]Matei A, Cernica I, Cadar O, et al. *Int. J. Mater. Form.*, **2008**,**1**(0):767-770

[36]Ardelean I, Cora S. *J. Mater. Sci. Mater. Elec*., **2008**,**19**(6): 584-588

[37]Chen L, Li L, Li G. *J. Alloys Compd*., **2008**,**464**(1/2):532-536

[38]Villa A L, Caro C A, Correa C M d. *J. Mol. Catal. A*: *Chem*., **2005**,**228**(1/2):233-240

[39]Zhang L M, Lu W C, Feng Y L, et al. *Acta Physico-Chimica Sinica*, **2008**,**24**(12):2257-2262

[40]Sun W, Liu W L, Hu Y H. *J. Cent. South Univ. Tech*., **2008**,**15**(3):373-377

[41]Mali A, Ataie A. *Ceram. Int*., **2004**,**30**(7):1979-1983